

Bound states of a fermion-dyon system

A.Yu. Loginov^{1,a}

¹Laboratory of Applied Mathematics and Theoretical Physics, Tomsk State University of Control Systems and Radioelectronics, 634050 Tomsk, Russia

Received: date / Accepted: date

Abstract The bound states of fermions in the external field of an Abelian dyon are studied here both analytically and numerically. Their existence is due to the dyon's electric charge resulting from a polarization of the fermionic vacuum. The configuration of the dyon's field is not invariant under P or CP transformations. The dependence of the energy levels of the fermion-dyon system on a parameter of CP violation is investigated. The absence of P invariance results in nonzero electric dipole moments of the bound fermionic states. These depend nontrivially on the parameter of CP violation. The bound fermionic states also possess nonzero magnetic dipole moments. Unlike the electric dipole moments, the magnetic dipole moments are practically independent of the parameter of CP violation. In addition, the magnitudes of the electric dipole moments significantly exceed those of the magnetic dipole moments.

1 Introduction

The interaction of fermions with the Dirac monopole [1, 2] has been discussed by many authors [3–33]. One reason for this is that the characteristic features of the fermion-monopole system distinguish it from the hydrogen atom. In particular, unlike a spherically symmetric electric field, the monopole's magnetic field is not invariant (it changes sign) under P transformation. As a result, bound states of the fermion-monopole system may possess nonzero electric dipole moments [13, 14]. Another important feature is the absence of the centrifugal barrier in the state with the minimal angular momentum, which results in the fermions easily reaching the location of the monopole. Due to this, the

Dirac Hamiltonian is not self-adjoint on the subspace of wave functions with the minimal angular momentum, which is unacceptable. To solve this problem, an infinitesimally small “extra” magnetic moment is added to the Dirac fermion [11, 12, 14], which is equivalent to a boundary condition at $r = 0$.

However, this boundary condition is not the most general, and there is a one-parameter family of appropriate boundary conditions [13, 15], corresponding to the existence of θ vacua. Unlike the magnetic monopole's field, these boundary conditions are not CP -invariant. For massive fermions, this leads to a violation of CP invariance of the fermion-monopole system. It was shown in [16] that this violation leads to a polarization of the fermionic vacuum in the vicinity of the monopole, as a result of which the monopole becomes a dyon whose electric charge is determined by the Witten formula [35]. The long-distance asymptotics of the dyon's electric potential is Coulombic, but not its short-distance asymptotics.

The fermion-monopole system has a single bound state [13, 15] in a specified region of the parameter θ . This state possesses the minimal angular momentum, and is, in general, tightly bound. The attractive Coulomb asymptotics of the dyon's electric potential completely changes this picture. Like the hydrogen atom, the fermion-dyon system has an infinite number of loosely bound states for each value of the angular momentum including the minimal value. As with a purely Coulomb fermion-dyon system [25–28], the energy spectrum of these loosely bound states is hydrogen-like. However, in contrast to [25–28], a twofold degeneracy of the energy levels is removed already at the quantum mechanical level.

In general, the bound fermionic states possess both electric and magnetic dipole moments. The exception

^ae-mail: a.yu.loginov@tusur.ru

is the bound states with the minimal angular momentum. Their magnetic dipole moments vanish in any case, whereas their electric dipole moments vanish only if the minimal angular momentum is zero. The electric dipole moments depend nontrivially on the parameter θ , whereas the magnetic dipole moments are practically independent of it. The magnitudes of the electric dipole moments significantly exceed those of the magnetic dipole moments.

This paper is structured as follows. In Section 2, we briefly describe some properties of the fermion-monopole system. In Section 3, we describe the polarization of the fermionic vacuum in the vicinity of the monopole and the characteristics of the induced electric charge distribution. In Section 4, we study the bound fermionic states arising due to the induced electric charge of the dyon. We consider separately the bound fermionic states with the minimal and nonminimal angular momenta. In Sections 5 and 6, we study the electric and magnetic dipole moments of the bound fermionic states, respectively. In the last section, we briefly list the features of the fermion-dyon system and summarise the results obtained in the present work.

Throughout this paper, the natural units $c = 1$ and $\hbar = 1$ are used.

2 Some properties of the fermion-monopole system

The dynamics of a fermion in a fixed Abelian monopole field is determined by the Dirac equation

$$i\partial_t\psi = H\psi, \quad (1)$$

where the Hamiltonian

$$H = \boldsymbol{\alpha} \cdot (-i\nabla - e\mathbf{A}) + \beta M, \quad (2)$$

the matrices

$$\alpha^i = \gamma^0\gamma^i, \quad \beta = \gamma^0, \quad (3)$$

and we use the Dirac matrices in the standard representation

$$\gamma^0 = \begin{pmatrix} 1 & 0 \\ 0 & -1 \end{pmatrix}, \quad \gamma^i = \begin{pmatrix} 0 & \sigma^i \\ -\sigma^i & 0 \end{pmatrix}. \quad (4)$$

In Eq. (1), we consider the monopole vector potential \mathbf{A} not as an ordinary vector field, but as a connection on a nontrivial $U(1)$ bundle over $R^3/\{0\} \sim S^2$. Accordingly, the wave function ψ should be considered as a section rather than an ordinary function. This approach, proposed in [34], allows one to avoid an unwanted string singularity when describing the monopole.

To describe the monopole's vector potential we must consider the space outside of the monopole as the union of two overlapping regions R_a and R_b ,

$$R_a: r > 0, \quad 0 \leq \vartheta \leq \frac{\pi}{2} + \delta, \quad 0 \leq \varphi < 2\pi, \quad (5a)$$

$$R_b: r > 0, \quad \frac{\pi}{2} - \delta \leq \vartheta \leq \pi, \quad 0 \leq \varphi < 2\pi, \quad (5b)$$

where the angle δ is in the range $(0, \pi/2)$. Then, in the regions R_a and R_b , the monopole vector potential is chosen to be

$$\mathbf{A}^{(a)} = -\frac{g}{r} \frac{\mathbf{r} \times \mathbf{n}}{r + \mathbf{r} \cdot \mathbf{n}} \quad (6)$$

and

$$\mathbf{A}^{(b)} = \frac{g}{r} \frac{\mathbf{r} \times \mathbf{n}}{r - \mathbf{r} \cdot \mathbf{n}}, \quad (7)$$

respectively, where g is the monopole's magnetic charge and the unit vector $\mathbf{n} = (0, 0, 1)$. Note that both $\mathbf{A}^{(a)}$ and $\mathbf{A}^{(b)}$ are nonsingular in their domains of definition R_a and R_b . In the region of overlap $R_a \cap R_b$, the two potentials are related by a gauge transformation

$$A_\mu^{(a)} = A_\mu^{(b)} + \frac{i}{e} S_{ab} \partial_\mu S_{ab}^{-1}, \quad (8)$$

where the transition function

$$S_{ab} = e^{2ieg\varphi}. \quad (9)$$

Similar to the connection \mathbf{A} , the wave section ψ is given by two wave functions ψ_a and ψ_b defined in the regions R_a and R_b , respectively. In the region R_a (R_b), the wave function ψ_a (ψ_b) satisfies the Dirac equation (1) with the vector potential $\mathbf{A}^{(a)}$ ($\mathbf{A}^{(b)}$). In the region $R_a \cap R_b$, the wave functions ψ_a and ψ_b are connected by the relation

$$\psi_a = S_{ab}\psi_b. \quad (10)$$

The necessity of the single-valuedness of the transition function S_{ab} in the region $R_a \cap R_b$ leads to the Dirac quantization condition [1]

$$q \equiv eg = \frac{n}{2}, \quad (11)$$

where n is an integer.

The Hamiltonian (2) commutes with the angular momentum operator

$$\mathbf{J} = \mathbf{r} \times (-i\nabla - e\mathbf{A}) + \mathbf{S} - q\frac{\mathbf{r}}{r}, \quad (12)$$

where the spin operator

$$\mathbf{S} = \frac{1}{2} \begin{pmatrix} \boldsymbol{\sigma} & 0 \\ 0 & \boldsymbol{\sigma} \end{pmatrix}. \quad (13)$$

A characteristic feature of operator (12) is the presence of the radial term qr/r , which leads to a number of

unusual properties of the fermion-monopole system. In particular, it follows from Eq. (12) and the addition rule for angular momenta that the minimum value of the fermion angular momentum is $j = |q| - 1/2$. Hence, for the fundamental Dirac monopole ($n = 1, q = 1/2$), the minimum value of the fermion angular momentum is zero. Furthermore, a fermion-monopole system with an odd (even) n can possess only integer (half-integer) angular momenta.

2.1 Properties of the fermion-monopole system under the discrete transformations of QFT

Now we shall investigate the properties of the fermion-monopole system under the discrete transformations of QFT. First, we note that the two components of the connection \mathbf{A} satisfy the relation

$$\mathbf{A}^{(a,b)}(\mathbf{x}) = \mathbf{A}^{(b,a)}(-\mathbf{x}). \quad (14)$$

Then, it follows from Eqs. (6), (7), and (14) that under P transformation, $\mathbf{A}^{(a,b)}(\mathbf{x}) \rightarrow \mathbf{A}^{P(a,b)}(\mathbf{x})$, where

$$\mathbf{A}^{P(a,b)}(\mathbf{x}) = -\mathbf{A}^{(b,a)}(-\mathbf{x}) = -\mathbf{A}^{(a,b)}(\mathbf{x}). \quad (15)$$

We see that P transformation is equivalent to the reversal of sign $g \rightarrow -g$ of the magnetic charge of the monopole. Using Eqs. (1), (2), (15), and the properties of the Dirac matrices, we obtain the transformation law for the fermion wave functions $\psi_{(a,b)}$ under P transformation

$$\psi_{(a,b)}^P(t, \mathbf{x}) = \eta_P \gamma^0 \psi_{(b,a)}(t, -\mathbf{x}), \quad (16)$$

where η_P is a phase factor. The P transformation is not a symmetry of the fermion-monopole system, which distinguishes it from the hydrogen atom. Rather, it transforms the fermion (antifermion) wave function in the external field of the monopole of charge g to the fermion (antifermion) wave function in the external field of the monopole of charge $-g$.

Under C conjugation, the components of the connection \mathbf{A} are transformed just as under P transformation

$$\mathbf{A}^{(a,b)}(\mathbf{x}) \rightarrow \mathbf{A}^{C(a,b)}(\mathbf{x}) = -\mathbf{A}^{(a,b)}(\mathbf{x}), \quad (17)$$

whereas the fermion wave functions are transformed as

$$\psi_{(a,b)}^C(t, \mathbf{x}) = \eta_C \gamma^2 \psi_{(a,b)}^*(t, \mathbf{x}), \quad (18)$$

where η_C is a phase factor. We see that like P transformation, C conjugation is not a symmetry of the fermion-monopole system. Instead, it transforms the fermion (antifermion) wave function in the external field

of the monopole of charge g to the antifermion (fermion) wave function in the external field of the monopole of charge $-g$.

Combining Eqs. (15) and (17), we conclude that CP inversion leaves the monopole's vector potential unchanged. At the same time, Eqs. (16) and (18) tell us that under CP , the wave function $\psi_{(a,b)}(t, \mathbf{x}) \rightarrow \psi_{(a,b)}^{CP}(t, \mathbf{x})$, where

$$\psi_{(a,b)}^{CP}(t, \mathbf{x}) = \eta_{CP} \alpha_2 \psi_{(b,a)}^*(t, -\mathbf{x}), \quad (19)$$

the CP phase $\eta_{CP} = -\eta_C \eta_P^*$, and the matrix $\alpha_2 = \gamma^0 \gamma^2$. Since CP inversion does not change the vector potential of the monopole, it could be a symmetry of the fermion-monopole system transforming its fermion (antifermion) states to antifermion (fermion) ones. However, we shall see later that in the general case, CP is not a symmetry of the fermion-monopole system.

2.2 The fermion-monopole system in a state with the lowest angular momentum $j = |q| - 1/2$

It was shown in [11] that the angular momentum operator (12) has three types of eigensections. We focus on the eigensection of the third type, since it describes the lowest partial wave with $j = |q| - 1/2$. The fermion wave section is written as

$$\psi_{jm}^{(3)}(t, \mathbf{x}) = \frac{1}{r} \chi(r) \otimes \eta_{jm}(\vartheta, \varphi) e^{-iEt}, \quad (20)$$

where the radial part is

$$\chi(r) = \begin{bmatrix} f(r) \\ g(r) \end{bmatrix}, \quad (21)$$

the eigensection of the third type is

$$\eta_{jm} = \begin{bmatrix} -\left(\frac{j-m+1}{2j+2}\right)^{1/2} Y_{q,|q|,m-1/2} \\ \left(\frac{j+m+1}{2j+2}\right)^{1/2} Y_{q,|q|,m+1/2} \end{bmatrix}, \quad (22)$$

the angular momentum $j = |q| - 1/2$, and the z projection m of the angular momentum is in the range $[-|q| + 1/2, |q| - 1/2]$. The monopole spherical harmonics $Y_{q,l,\mu}(\vartheta, \varphi)$ entering into Eq. (22) were defined in [9], and their properties were derived in [10]. In Eq. (20), the nontrivial topology of the monopole $U(1)$ bundle is completely reflected in the eigensection $\eta_{jm}(\vartheta, \varphi)$, whereas $\chi(r)$ is an ordinary two-component wave function defined on the interval $[0, \infty)$.

Substituting Eq. (20) into Eq. (1) and using the properties [11] of the eigensection $\eta_{jm}(\vartheta, \varphi)$, we reduce

the Dirac equation to a system of two differential equations for the radial functions

$$H\chi(r) = E\chi(r), \quad (23)$$

where the reduced Hamiltonian is

$$H = -i\frac{q}{|q|}\tilde{\gamma}_5\frac{d}{dr} + M\tilde{\beta} \quad (24)$$

with the matrices

$$\tilde{\gamma}_5 = \begin{bmatrix} 0 & 1 \\ 1 & 0 \end{bmatrix} \quad \text{and} \quad \tilde{\beta} = \begin{bmatrix} 1 & 0 \\ 0 & -1 \end{bmatrix}. \quad (25)$$

Using Eqs. (15) – (22), it can be shown that the effects of P and CP transformations on the two-component radial wave function χ are

$$\chi \xrightarrow{P} \chi^P = \tilde{\beta}\chi, \quad q \xrightarrow{P} -q, \quad E \xrightarrow{P} E \quad (26)$$

and

$$\chi \xrightarrow{CP} \chi^{CP} = i\tilde{\gamma}_5\chi^*, \quad q \xrightarrow{CP} q, \quad E \xrightarrow{CP} -E, \quad (27)$$

respectively. Eq. (26) tells us that we may restrict ourselves to the case $q > 0$, since the solutions for $q < 0$ can be obtained by the parity transformation.

The reduced Hamiltonian (24) corresponds to the state with the lowest possible angular momentum $j = |q| - 1/2$. Its characteristic feature is the absence of a centrifugal barrier at small r , which is a consequence of the presence of the additional term $-q\mathbf{r}/r$ in Eq. (12). The two-component radial wave functions $\chi(r)$ are defined on the interval $[0, \infty)$, and their inner product is defined by

$$(\chi_1, \chi_2) = \int_0^\infty \chi_1^\dagger(r) \chi_2(r) dr. \quad (28)$$

To correspond to a physical observable, the Hamiltonian (24) must be Hermitian with respect to this inner product, i.e.,

$$\begin{aligned} (\chi_1, H\chi_2) - (H\chi_1, \chi_2) &= i\chi_1^\dagger(0) \tilde{\gamma}_5\chi_2(0) = \\ &= i[f_1^*(0)g_2(0) + g_1^*(0)f_2(0)] = 0, \end{aligned} \quad (29)$$

where we have assumed that χ_1 and χ_2 vanish sufficiently rapidly at infinity.

The simple structure of the Hamiltonian (24) allows us to obtain the general solution to Eq. (23) in an analytical form

$$\chi_E(r) = c_1\chi_E^{(1)}(r) + c_2\chi_E^{(2)}(r), \quad (30)$$

where

$$\chi_E^{(1)}(r) = \begin{bmatrix} \frac{ik}{E-M} \sin(kr) \\ \cos(kr) \end{bmatrix}, \quad (31)$$

$$\chi_E^{(2)}(r) = \begin{bmatrix} \cos(kr) \\ \frac{ik}{E+M} \sin(kr) \end{bmatrix}, \quad (32)$$

$$E = \pm(k^2 + M^2)^{1/2}, \quad (33)$$

and it is assumed that $k > 0$. It follows from Eqs. (30) – (32) that $\chi_E^T(0) = (c_1, c_2)$, and it does not vanish except for the trivial case $c_1 = c_2 = 0$. Hence, in general, the Hermiticity condition (29) is not satisfied, and the Hamiltonian is not a self-adjoint operator on the states with the lowest angular momentum $j = |q| - 1/2$. Furthermore, it can be shown that the radial component of the fermion current $j^\mu = \bar{\psi}^{(3)}\gamma^\mu\psi^{(3)}$ is $j_r = \text{Re}[c_1c_2^*]/(2\pi r^2)$. It follows that the fermion flux through a spherical surface surrounding the monopole is $\Phi = 2\text{Re}[c_1c_2^*]$, and is not equal to zero in the general case. This is equivalent to the presence of a source of fermions (or antifermions) at the origin and contradicts the unitarity condition.

Nevertheless, the unitarity problem will be solved and the Hermiticity condition (29) will be satisfied provided that for any two solutions $\chi_1^T(r) = (f_1(r), g_1(r))$ and $\chi_2^T(r) = (f_2(r), g_2(r))$ of Eq. (23) (including the coincident case of $\chi_1(r) = \chi_2(r)$), the sesquilinear combination $f_1^*(0)g_2(0) + g_1^*(0)f_2(0)$ vanishes, which is equivalent to the relation $[f_1(0)/g_1(0)]^* = -f_2(0)/g_2(0)$. It follows that any solution $\chi^T(r) = (f(r), g(r))$ of Eq. (23) must satisfy [13, 15]

$$\frac{f(0)}{g(0)} = i \tan \left[\frac{\theta}{2} + \frac{\pi}{4} \right], \quad (34)$$

where the parametric angle $\theta \in (-\pi, \pi)$. Thus, the formal Hamiltonian (24) admits a one-parameter family of self-adjoint extensions [13, 15] provided that its eigenfunctions satisfy Eq. (34).

It can be easily checked that under CP inversion (27), the parameter θ changes sign

$$\theta \xrightarrow{CP} -\theta. \quad (35)$$

It follows that in the general case, CP is not a symmetry of the fermion-monopole system [16]. The only exceptions are for the values of the parameter $\theta = 0$, and $\pm\pi$. In the latter case, the values of $\theta = \pm\pi$ correspond to the same state, since $\tan[-\pi/2 + \pi/4] = \tan[\pi/2 + \pi/4] = -1$ and condition (34) remains unchanged.

Note that there are no problems related to the Hermiticity and unitarity for states of the fermion-monopole system with the angular momentum $j > |q| - 1/2$. This is because there is a centrifugal barrier in this case, and therefore the radial wave functions vanish at the origin.

2.3 Eigenfunctions of the Hamiltonian in the case of massive fermions

In the case of massive fermions, the reduced Hamiltonian (24) possesses the following eigenfunctions of the

continuous spectrum [16]:

$$u_{k\theta}(r) = \frac{2^{1/2}k}{[E(E - M \sin(\theta))]^{1/2}} \times \left[\cos\left(\frac{\theta}{2} + \frac{\pi}{4}\right) \chi_E^{(1)}(r) + i \sin\left(\frac{\theta}{2} + \frac{\pi}{4}\right) \chi_E^{(2)}(r) \right] \quad (36)$$

for $E = (k^2 + M^2)^{1/2}$, and

$$v_{k\theta}(r) = \frac{2^{1/2}k}{[|E|(|E| + M \sin(\theta))]^{1/2}} \times \left[\cos\left(\frac{\theta}{2} + \frac{\pi}{4}\right) \chi_E^{(1)}(r) + i \sin\left(\frac{\theta}{2} + \frac{\pi}{4}\right) \chi_E^{(2)}(r) \right] \quad (37)$$

for $E = -(k^2 + M^2)^{1/2}$. In addition, there is also a bound state [13, 15] of the discrete spectrum with the energy $E = M \sin(\theta)$, provided that $\cos(\theta) < 0 \Leftrightarrow \theta \in [-\pi, -\pi/2) \cup (\pi/2, \pi]$. The radial wave function of this state is

$$B_\theta(r) = \begin{bmatrix} i \sin\left(\frac{\theta}{2} + \frac{\pi}{4}\right) \\ \cos\left(\frac{\theta}{2} + \frac{\pi}{4}\right) \end{bmatrix} \sqrt{2\kappa} e^{-\kappa r}, \quad (38)$$

where the parameter $\kappa = M |\cos(\theta)|$.

The eigenfunctions (36) – (38) satisfy

$$(u_{k\theta}, u_{k'\theta}) = 2\pi\delta(k - k'), \quad (39a)$$

$$(v_{k\theta}, v_{k'\theta}) = 2\pi\delta(k - k'), \quad (39b)$$

$$(B_\theta, B_\theta) = 1, \quad (39c)$$

while all other inner products vanish. We see that eigenfunctions (36) – (38) form a complete orthonormal system on the half-line $r \geq 0$. Finally, it is easily shown that under CP inversion

$$u_{k\theta} \xrightarrow{CP} u_{k\theta}^{CP} = i\tilde{\gamma}_5 u_{k\theta}^* = v_{k-\theta}, \quad (40a)$$

$$v_{k\theta} \xrightarrow{CP} v_{k\theta}^{CP} = i\tilde{\gamma}_5 v_{k\theta}^* = u_{k-\theta}, \quad (40b)$$

$$B_\theta \xrightarrow{CP} B_\theta^{CP} = i\tilde{\gamma}_5 B_\theta^* = B_{-\theta}, \quad (40c)$$

in accordance with Eq. (35).

3 Polarization of the fermionic vacuum in the vicinity of the magnetic monopole

It follows from Eqs. (40a) – (40c) that the fermion-monopole system is not CP -invariant, since the parameters $\pm\theta$ correspond to two different fermion-monopole systems. It was shown in [16] that this violation of CP

invariance results in a polarization of the fermionic vacuum in the vicinity of the monopole, with the result that the monopole becomes a dyon. The density of the induced electric charge is

$$\rho(r, \theta) = -\frac{qeM \sin(\theta)}{2\pi^2 r^2} \times \int_M^\infty \frac{\kappa \exp(-2\kappa r)}{(\kappa^2 - M^2)^{1/2} (\kappa + M \cos(\theta))} d\kappa. \quad (41)$$

Although the integral in Eq. (41) cannot be calculated analytically in the general case, the induced electric charge $Q = 4\pi \int_0^\infty \rho(r, \theta) r^2 dr$ can be obtained in an analytical form [16]

$$Q = -\frac{qe\theta}{\pi}. \quad (42)$$

For a monopole with minimal magnetic charge ($n = 1$, $q = 1/2$), Eq. (42) is precisely the Witten formula [35, 36]. We conclude that for $M > 0$, the Abelian magnetic monopole becomes a dyon due to the polarization of the fermionic vacuum.

Using Eq. (41), one can derive several analytical expressions related to the spatial distribution of the dyon's electric charge. In particular, the mean radius of the charge distribution is $\langle r \rangle_{\text{el}} = 4\pi Q^{-1} \int_0^\infty r \rho(r, \theta) dr$ and the mean radius squared of the charge distribution is $\langle r^2 \rangle_{\text{el}} = 4\pi Q^{-1} \int_0^\infty r^2 \rho(r, \theta) dr$. Both can be expressed in terms of elementary functions:

$$\langle r \rangle_{\text{el}} = \frac{1}{2M \cos(\theta)} \left(\frac{\pi \sin(\theta)}{2\theta} - 1 \right) \quad (43)$$

and

$$\langle r^2 \rangle_{\text{el}} = \frac{1}{4M^2 \cos^2(\theta)} \left(2 - \frac{\pi \sin(\theta)}{\theta} + \frac{\sin(2\theta)}{\theta} \right). \quad (44)$$

Using Eqs. (43) and (44), we then obtain the expression for the dispersion $D_{\text{el}} = \langle r^2 \rangle_{\text{el}} - \langle r \rangle_{\text{el}}^2$ of the charge distribution

$$D_{\text{el}} = \frac{1}{4M^2 \cos^2(\theta)} \left(1 - \frac{\pi^2 \sin^2(\theta)}{4\theta^2} + \frac{\sin(2\theta)}{\theta} \right). \quad (45)$$

The electric potential corresponding to the charge density (41) can be written as

$$A_0(r) = -\frac{qe\theta}{\pi r} + \frac{qeM \sin(\theta)}{\pi r} \times \int_M^\infty \frac{(e^{-2\kappa r} + 2\kappa r \text{Ei}(-2\kappa r))}{(\kappa^2 - M^2)^{1/2} (\kappa + M \cos(\theta))} d\kappa, \quad (46)$$

where $\text{Ei}(x)$ is the exponential integral function [38]. The definite integrals in Eqs. (41) and (46) cannot be found in an analytical form in the general case. We can, however, obtain the asymptotics of the electric charge

density (41) and electric potential (46) using standard methods:

$$\rho(r, \theta) \sim \frac{qeM \sin(\theta)}{2\pi^2 r^2} \ln(Mr), \quad (47)$$

$$A_0(r, \theta) \sim -\frac{qeM \sin(\theta)}{\pi} (1 - \ln(Mr))^2 \quad (48)$$

for $r \rightarrow 0$, and

$$\rho(r, \theta) \sim -\frac{qeM \tan(\theta/2)}{2\pi^2 r^2} \left(\frac{\pi}{4Mr}\right)^{1/2} e^{-2Mr}, \quad (49)$$

$$A_0(r, \theta) \sim -\frac{qe\theta}{\pi r} + \frac{qe \tan(\theta/2)}{\pi r} \frac{\sqrt{\pi}}{4} \frac{e^{-2Mr}}{(Mr)^{3/2}} \quad (50)$$

for $r \rightarrow \infty$. The Eqs. (47) – (50) become inapplicable for $\theta = \pm\pi$. In this case, we can obtain an analytical form of $\rho(r, \pm\pi)$ after an integration by parts

$$\rho(r, \pm\pi) = \mp \frac{qeM}{2\pi r^2} e^{-2Mr}. \quad (51)$$

The electric potential $A_0(r, \pm\pi)$ can also be obtained in an analytical form

$$A_0(r, \pm\pi) = \mp \frac{qe}{r} [1 - e^{-2Mr} + 2Mr\Gamma(0, 2Mr)], \quad (52)$$

where $\Gamma(0, 2Mr)$ is the incomplete gamma function [38].

Eqs. (47), (49), and (51) tell us that the radial density $4\pi r^2 \rho(r)$ has an integrable singularity at the origin and tends to zero exponentially as $r \rightarrow \infty$. Further, the characteristic size (43) of the charge distribution is on the order of the inverse fermion mass M^{-1} . This smeared charge distribution results in the potential $A_0(r)$ having only a weak logarithmic singularity at the origin. In contrast, the point-like ($\propto \delta(\mathbf{x})$) distribution of the electric charge leads to a pole singularity ($\propto r^{-1}$) of the potential $A_0(r)$. As a result, the electrostatic energy of the charge distribution surrounding the magnetic monopole is finite and can be written as

$$E_{\text{el}} = q^2 \alpha M \tilde{E}_{\text{el}}(\theta), \quad (53)$$

where $\alpha = e^2$ is the fine structure constant and $\tilde{E}_{\text{el}}(\theta)$ is an even dimensionless function. For example, the electrostatic energy corresponding to the parameter $\theta = \pm\pi$ is

$$E_{\text{el}}(\pm\pi) = q^2 \alpha M \ln(4). \quad (54)$$

Similar to $\tilde{E}_{\text{el}}(\theta)$, we define the dimensionless mean radius $\langle \tilde{r} \rangle_{\text{el}} = M \langle r \rangle_{\text{el}}$ and the scaled electric charge $\tilde{Q} = Q/(qe) = -\theta/\pi$. We also define the dimensionless standard deviation $\tilde{\sigma}_{\text{el}} = M\sigma_{\text{el}} = MD_{\text{el}}^{1/2}$, which characterizes the deviation from the mean radius. Figure 1 shows the dependence of these dimensionless quantities on the parameter θ . The most interesting feature

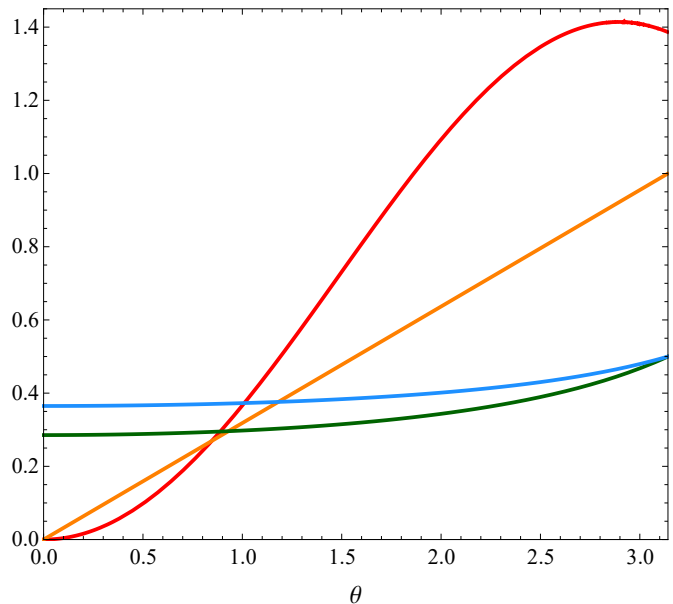


Fig. 1 Dependence of the dimensionless quantities \tilde{E}_{el} (red curve), $|\tilde{Q}|$ (orange curve), $\langle \tilde{r} \rangle_{\text{el}}$ (green curve), and $\tilde{\sigma}_{\text{el}}$ (blue curve) on the parameter θ

is that $\tilde{E}_{\text{el}}(\theta)$ is not a monotonically increasing function of θ . Instead, $\tilde{E}_{\text{el}}(\theta)$ reaches a global maximum approximately equal to 1.41 at $\theta \approx 2.9$. Hence, the electrostatic energy (53) is not a monotonically increasing function of the magnitude of the electric charge $|Q|$, since the latter is related to θ by the linear relation $|Q| = \text{sgn}(\theta) |q| e\theta/\pi$. This is because the effective size of charge distribution (41), which is characterized by the parameters $\langle \tilde{r} \rangle_{\text{el}}$ and $\tilde{\sigma}_{\text{el}}$, increases monotonically with an increase in θ . As a result, for $\theta \gtrsim 2.9$, the effect of increasing the spatial size of the charge distribution overpowers the effect of increasing the magnitude of the electric charge, and the electrostatic energy begins to decrease.

It should be noted that the values of $\theta = \pm\pi$ require special consideration, since the energy $E = M \sin(\theta)$ of the bound fermionic state vanishes in this case. Here we deal with the presence of the fermionic zero modes $B_{\pm\pi}$ in the external field of a topologically nontrivial field configuration (the monopole bundle). However, it follows from Eqs. (38) and (40c) that

$$B_{\pi} \xrightarrow{CP} B_{-\pi} = -B_{\pi}. \quad (55)$$

We see that the zero modes B_{π} and $B_{-\pi}$ differ only in the sign (the phase factor), and therefore are equivalent to each other, as well as the values $\pm\pi$ of the parameter θ .

Now we consider the case $q = 1/2$, for which the angular momentum $j = 0$, and hence there is no angular momentum degeneracy. However, the presence of

the fermionic zero mode $B_{\pm\pi}$ still leads to a twofold degeneracy of the fermion-dyon system when the parameter $\theta = \pm\pi$, since the fermionic zero mode can be either filled or unfilled [37]. Note in this regard that Eq. (41) was obtained under the assumption that the bound fermionic state with the positive (negative) energy is unfilled (filled). For reasons of continuity, it follows that the value of $\theta = \pi (-\pi)$ corresponds to the unfilled (filled) fermionic zero mode. Then Eq. (42) tells us that the electric charge of the fermion-dyon system with the unfilled (filled) zero mode is $Q_u = -e/2$ ($Q_f = e/2$). Hence, the corresponding fermion number is $N_u = -1/2$ ($N_f = 1/2$), and is half-integral, as is the case for the fermion-kink system [37]. We see that $Q_f - Q_u = e$ and $N_f - N_u = 1$, as it should be. The similar situation occurs when $|q| > 1/2$. In this case, the angular momentum $j = |q| - 1/2 > 0$, and the multiplicity of the degeneracy is $2(2j + 1) = 4|q|$.

4 Bound states of the fermion-dyon system

From the previous section, we know that the polarization of the fermionic vacuum in the vicinity of the Abelian magnetic monopole results in a localized spherically-symmetric distribution of the electric charge in the vicinity of the monopole [16]. Thus, the magnetic monopole becomes a dyon with the electric charge defined by the Witten formula (42). The corresponding electric potential (46) has the long-range Coulomb asymptotics (50). For positive q , this asymptotics is attractive for fermions (antifermions), provided that $\theta > 0$ ($\theta < 0$). Then, it follows from the general consideration of [39] that due to the long-range Coulomb asymptotics (50), there are an infinite number of bound (anti)fermionic states for any value j of the angular momentum. We conclude that the induced electric charge (42) leads to the appearance of new bound fermionic states of the fermion-dyon system. In addition, the induced electric charge leads to a modification of the already existing bound fermionic state (38).

4.1 Bound fermionic states with the minimal angular momentum $j = |q| - 1/2$

The presence of the electric charge leads to modification of the reduced Hamiltonian (24) which now takes the form

$$H = -i\frac{q}{|q|}\tilde{\gamma}_5\frac{d}{dr} + M\tilde{\beta} + eA_0\mathbb{I}, \quad (56)$$

where \mathbb{I} is the two-dimensional identity matrix. Let us determine how the presence of the electric potential A_0

in Eq. (56) affects the behaviour of solutions (36) – (38) in the vicinity of $r = 0$. According to Eq. (48), the electric potential increases indefinitely as $r \rightarrow 0$. Hence, we can neglect the mass term $M\tilde{\beta}$ in Eq. (56), and write the short distance asymptotics of the modified solution as

$$\tilde{u}_{k\theta}(r) \sim \exp\left[-ie\tilde{\gamma}_5\int_0^r A_0(s)ds\right]u_{k\theta}(r), \quad (57)$$

where $u_{k\theta}(r)$ is solution (36) corresponding to zero electric potential A_0 . The solutions (37) and (38) are modified similarly.

Using the short distance asymptotics (48) of the electric potential, one can show that the integral

$$e\int_0^r A_0(s)ds \sim -\frac{\alpha}{\pi}qM\sin(\theta)r[\ln(Mr)]^2 \quad (58)$$

as $r \rightarrow 0$. It follows that $\lim_{r \rightarrow 0} e\int_0^r A_0(s)ds = 0$, and therefore the exponential function in Eq. (57) tends to unity as $r \rightarrow 0$. This behaviour of the exponential function is a consequence of the weak (logarithmic) singularity of the electric potential A_0 at the origin.

Based on the above, we conclude that the presence of the electric potential A_0 in Eq. (56) does not lead to a radical change in the solutions (36) – (38) in the neighbourhood of $r = 0$. In particular, we conclude that $\tilde{u}_{k\theta}(0) = u_{k\theta}(0) \neq 0$, and that similar relations hold for solutions (37) and (38). It follows that the Hermiticity condition (29) and Eq. (34) remain satisfied even when the potential $A_0 \neq 0$.

The integral $\int_0^r A_0(s)ds$ vanishes in the limit of small r also if the potential $A_0 \sim r^{-\epsilon}$, where the exponent $\epsilon \in (0, 1)$. Therefore, all conclusions of the previous paragraph remain valid in this case too. In contrast, the integral diverges at the lower limit when the exponent $\epsilon \geq 1$. In this case, the exponential function in Eq. (57) oscillates unboundedly and does not tend to any limit as $r \rightarrow 0$. This behaviour corresponds to the situation of falling on the centre in QM and is unacceptable [39].

For example, for the Coulomb potential $A_0 = -Ze/r$, the solution to the Dirac equation $H\chi = E\chi$, where H is given by Eq. (56), can be expressed in terms of the confluent Heun function [38] and its derivative. The short distance asymptotics of this solution is

$$\chi(r) \sim \begin{pmatrix} c_1 e^{iZ\alpha \ln(Mr)} + c_2 e^{-iZ\alpha \ln(Mr)} \\ c_1 e^{iZ\alpha \ln(Mr)} - c_2 e^{-iZ\alpha \ln(Mr)} \end{pmatrix}, \quad (59)$$

where c_1 and c_2 are arbitrary complex constants. We see that as $r \rightarrow 0$, the solution oscillates with increasing frequency, which corresponds to falling of the fermion on the dyon's centre. As $r \rightarrow 0$, the asymptotics of the ratio of the radial functions is

$$\frac{f(r)}{g(r)} \sim 1 - \frac{2c_2}{c_2 - c_1 e^{2iZ\alpha \ln(r)}}. \quad (60)$$

Except for the two degenerate cases $c_1 = 0$ and $c_2 = 0$, the ratio (60) does not tend to a certain limit as $r \rightarrow 0$. In the two degenerate cases, this ratio is ∓ 1 and is real. We see that the asymptotics (59) is incompatible with the boundary condition (34).

It was shown in Section 2 that CP inversion leaves the vector potential of the monopole unchanged. Due to this, CP is a symmetry of the fermion-monopole system, provided that its angular momentum $j \geq |q| + 1/2$. At the same time, the boundary condition (34) is not invariant under CP , which changes sign of the parameter θ . Hence, CP is not a symmetry of the fermion-monopole system with the lowest angular momentum $j = |q| - 1/2$.

The situation changes when we consider the polarization of the fermionic vacuum, which is equivalent to the transformation of the monopole into a dyon. Since the electric charge of the dyon is nonzero, it possesses a radial electric field $E_r = -\partial_r A_0$ corresponding to the electric potential A_0 . Unlike the monopole's magnetic potential \mathbf{A} , the dyon's electric potential A_0 changes sign under CP inversion. Hence, CP transforms the original dyon into another one with the opposite electric charge. As a consequence, CP cannot be a symmetry of the fermion-dyon system even when its angular momentum $j \geq |q| + 1/2$.

Without considering the electric charge, the fermion-monopole system possesses the single bound (anti)fermionic state (38) existing due to the nontrivial boundary condition (34). Accounting for electric charge leads to corrections to the wave function of the bound state (38) and to its energy. These corrections can be calculated either numerically or using the perturbation theory. In the latter case, the first order correction to the energy is

$$\Delta E^{(1)} = (B_\theta, \Delta H B_\theta), \quad (61)$$

where the perturbation $\Delta H = eA_0 \mathbb{I}$. Using Eqs. (38) and (46), and applying analytical and approximate methods, we obtain an approximate analytical expression for the first-order energy correction

$$\begin{aligned} \Delta E^{(1)} \approx & -2Mq \frac{\alpha}{\pi} \theta \cos(\theta) \ln[-\cos(\theta)] \\ & + \frac{Mq \alpha}{12 \pi} \operatorname{sgn}(\theta) \cos(\theta) \{12\pi(1 + \ln(2)) \\ & + 12(\ln(4) - 5) \cos(\theta) - \pi \cos^2(\theta)\}, \end{aligned} \quad (62)$$

where $|\theta| \in [\pi/2, \pi]$. We see that the correction to the energy $E = M \sin(\theta)$ of the bound state (38) is small, since the fine structure constant $\alpha \approx 1/137 \ll 1$. Furthermore, it changes its sign under CP inversion at which $\theta \rightarrow -\theta$.

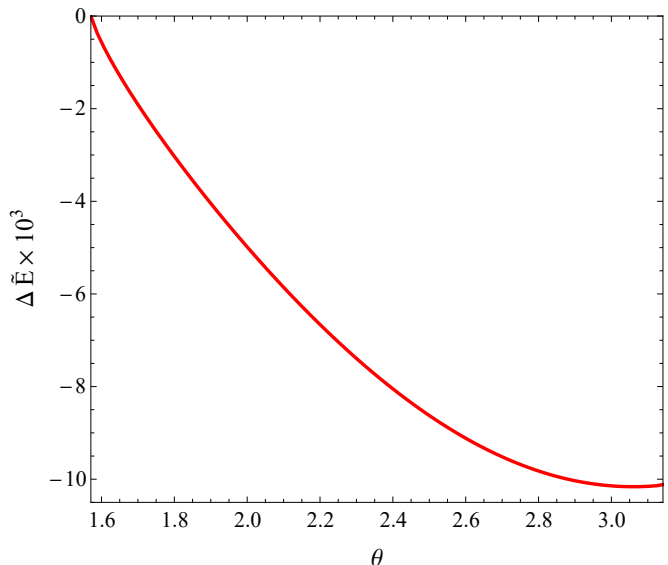


Fig. 2 Dependence of the correction $\Delta \tilde{E} = \Delta E/M$ to the energy of bound state (38) on the parameter θ . The correction corresponds to the parameters $\alpha = 1/137$ and $q = 1/2$

Figure 2 shows the dependence of the correction to the energy of the bound state (38) on the parameter θ . The correction was found by numerically solving the first-order system $H\chi = E\chi$ with the perturbed Hamiltonian (56). Note that the curve $\Delta E^{(1)}$ obtained using Eqs. (61) and (62) is visually indistinguishable from that shown in Fig. 2. This is because the difference $\Delta E - \Delta E^{(1)}$ is proportional to α^2 , where the fine structure constant $\alpha \approx 1/137 \ll 1$. It follows from Fig. 2 that the presence of the electric charge increases the binding energy of the fermion-dyon system because the signs of the electric charges of the dyon and fermion are opposite. As a result, the curve $E(\theta) = M \sin(\theta) + \Delta E(\theta)$ crosses zero not at the point $\theta = \pi$ as in the unperturbed case $\Delta E(\theta) = 0$, but at the nearby point $\theta \approx \pi - 2.76q\alpha$.

Eq. (62) tells us that in the neighbourhood of $\theta = \pi/2$, the correction $\Delta E^{(1)}$ can be written as

$$\Delta E^{(1)} \approx \alpha q M \delta (\ln(\delta/2) - 1), \quad (63)$$

where the parameter $\delta = \theta - \pi/2 > 0$. On the other hand, the binding energy of the unperturbed bound state (38) is

$$E_u^{(b)} = M (\sin(\pi/2 + \delta) - 1) \approx -M\delta^2/2. \quad (64)$$

From Eqs. (63) and (64), it follows that the correction (63) exceeds the unperturbed binding energy (64) in the magnitude provided that $\pi/2 < \theta \lesssim \pi/2 - 2\alpha q \ln(\alpha)$. We see that in this small neighbourhood of θ , the role of the dyon's electric charge becomes comparable to that of the boundary condition (34).

Besides the corrections to the already existing bound state (38), the electric charge of the dyon gives rise to new bound states with the angular momentum $j = |q| - 1/2$. Indeed, at large distances, the electric potential A_0 is attractive and has long-range Coulomb asymptotics (50). In accordance with the considerations of [39], this should result in the existence of an infinite number of bound fermionic (antifermionic) states for positive (negative) θ . In contrast to the state (38), these states are loosely bound due to the smallness of the fine structure constant $\alpha \approx 1/137$. Furthermore, these states exist in the range of $0 < |\theta| \leq \pi$, whereas the bound state (38) exists only if $\pi/2 < |\theta| \leq \pi$.

To find the wave functions and energies of these bound states, we must solve an eigenvalue problem. The feature of our case is that the radial wave functions $f(r)$ and $g(r)$ are nonzero at $r = 0$ because of the boundary condition (34). This inhomogeneous boundary condition complicates the solution of the eigenvalue problem. To avoid this, we introduce the combination $F(r) = f(r) - i \tan[\theta/2 + \pi/4] g(r)$ for which $F(0) = 0$. We define the dimensionless radial function

$$\phi(r) = [E - M \sin(\theta) - eA_0(r)]^{-1/2} F(r), \quad (65)$$

which satisfies the homogeneous boundary condition $\phi(0) = 0$. Then, we reduce the first-order system $H\chi = E\chi$ with the perturbed Hamiltonian (56) to the second-order equation for the radial function $\phi(r)$

$$\phi'' + [-\varkappa^2 - V] \phi = 0, \quad (66)$$

where

$$V = 2eA_0E - \frac{eMA'_0 \cos(\theta)}{E - M \sin(\theta) - eA_0} + \frac{3}{4} \frac{e^2 A_0'^2}{(E - M \sin(\theta) - eA_0)^2} + \frac{1}{2} \frac{eA_0''}{E - M \sin(\theta) - eA_0} - e^2 A_0^2 \quad (67)$$

and $\varkappa^2 = M^2 - E^2$.

Eq. (66) formally coincides with a one-dimensional Schrödinger equation with the energy $-\varkappa^2$ and the potential V defined on the semi-infinite interval $r \geq 0$. The only difference is that the potential V depends on the fermion's energy E . A characteristic feature of the potential V is the absence of a centrifugal barrier. As a consequence, the potential $V \sim 1/(r^2 \ln(Mr))$ at short distances. At large distances, the potential V possesses a long-range asymptotics $\propto r^{-1}$. The nonanalytical behaviour of V at short distances excludes the possibility of an analytical solution of eigenvalue problem (66). To solve the eigenvalue problem, we use numerical methods implemented in the MATHEMATICA software package [40].

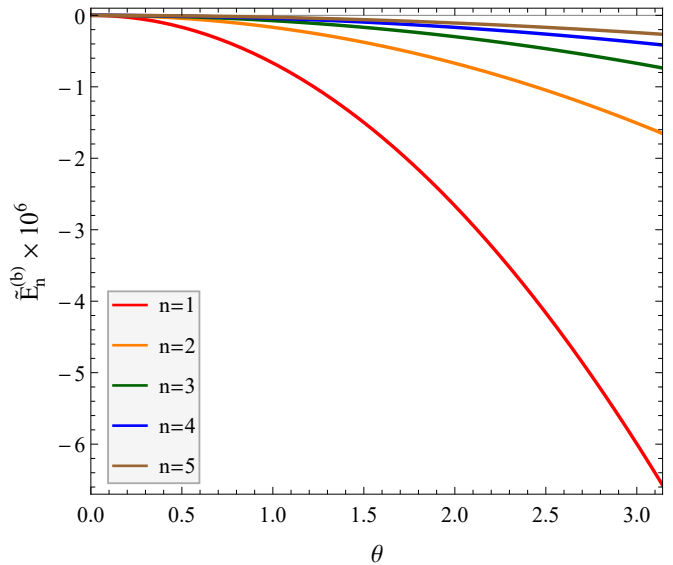


Fig. 3 Dependence of the dimensionless binding energy $\tilde{E}_n^{(b)} = (E_n - M)/M$ of the first five loosely bound fermionic states of the third type on the parameter θ . The curves correspond to the parameters $\alpha = 1/137$ and $q = 1/2$

Figure 3 shows the dependence of the binding energy $E_n^{(b)} = E_n - M$ of the first five bound fermionic states of the third type on the parameter θ . We consider the most realistic case of $\alpha = 1/137$ and $q = 1/2$. It was found numerically that all the curves $E_n^{(b)}(\theta)$ in Fig. 3 can be described with high accuracy by the quadratic dependence

$$E_n^{(b)}(\theta) \approx -a_n \theta^2, \quad (68)$$

where the radial quantum number $n = 1, 2, \dots$ is the number of zeros of either of the two radial functions f and g , and the coefficient $a_n \approx 6.5847 \times 10^{-6} n^{-2}$. We see, in Fig. 3, that the binding energies $E_n^{(b)}$ are much less than the fermion mass $M = 1$, and therefore the fermions are loosely bound and nonrelativistic. This is because the fine structure constant $\alpha = 1/137 \ll 1$, and the magnitude of electric charge of the dyon does not exceed $e/2$ when $q = 1/2$. On the contrary, the binding energy of state (38) is approximately $M(\sin(\theta) - 1)$, and, in the general case, this is of the same order as the fermion mass M . Hence, in this case, the fermion is tightly bound and relativistic. The reason is that the existence of the bound state (38) only depends on the boundary condition (34) and does not depend on the electric charge of the dyon.

4.2 Bound fermionic states with the angular momentum $j \geq |q| + 1/2$

We now consider the existence of bound fermionic states with angular momentum $j \geq |q| + 1/2$. It was shown in [11] that there are two types of fermionic states in this case. The states of the first type have the form

$$\psi_{jm}^{(1)}(t, \mathbf{x}) = \frac{1}{r} \begin{bmatrix} f(r) \xi_{jm}^{(1)}(\vartheta, \varphi) \\ g(r) \xi_{jm}^{(2)}(\vartheta, \varphi) \end{bmatrix} e^{-iEt}, \quad (69)$$

where the two-component angular momentum eigensections $\xi_{jm}^{(1)}(\vartheta, \varphi)$ and $\xi_{jm}^{(2)}(\vartheta, \varphi)$ were defined in [11]. The states of the second type are obtained from Eq. (69) by the permutation $\xi_{jm}^{(1)} \leftrightarrow \xi_{jm}^{(2)}$. In the following, we shall limit our discussion to states of the first type, since the properties of the two types of states are close enough.

Substituting Eq. (69) into the Dirac equation (1), we obtain the system of first-order equations for the radial wave functions

$$i(\partial_r - \mu r^{-1})f - (M + E - eA_0)g = 0, \quad (70)$$

$$i(\partial_r + \mu r^{-1})g + (M - E + eA_0)f = 0, \quad (71)$$

where the parameter $\mu = [(j + 1/2)^2 - q^2]^{1/2}$. We define dimensionless radial functions $u(r)$ and $v(r)$ as

$$u(r) = [E + M - eA_0(r)]^{-1/2} f(r), \quad (72a)$$

$$v(r) = [E - M - eA_0(r)]^{-1/2} g(r). \quad (72b)$$

Now we turn to the new radial functions and reduce the resulting first-order system to a second-order equation for one of the radial functions

$$u'' + [-\varkappa^2 - U]u = 0, \quad (73)$$

where

$$U = 2eA_0E - \frac{\mu(1-\mu)}{r^2} + \frac{e\mu A_0'}{E+M-eA_0} \frac{1}{r} + \frac{3}{4} \frac{e^2 A_0'^2}{(E+M-eA_0)^2} + \frac{1}{2} \frac{eA_0''}{E+M-eA_0} - e^2 A_0^2 \quad (74)$$

and $\varkappa^2 = M^2 - E^2$.

Similarly to Eq. (66), Eq. (73) formally coincides with a one-dimensional Schrödinger equation with energy $-\varkappa^2$ and an energy-dependent potential U defined on the semi-infinite interval $r \geq 0$. Using Eqs. (50) and (74), we obtain the large-distance asymptotics of the potential U

$$U \sim -2E \frac{z\alpha}{r} + \frac{\mu(\mu-1)}{r^2} - \frac{z^2\alpha^2}{r^2} + \frac{(\mu-1)z\alpha}{E+M} \frac{1}{r^3} + O\left[\frac{\alpha^2}{r^4}\right], \quad (75)$$

where the parameter $z = q\theta/\pi$. Similarly, using Eqs. (48) and (74), we obtain the short-distance asymptotics of U

$$U \sim \frac{\mu(\mu-1)}{r^2} + \frac{1-2\mu}{\ln(Mr)} \frac{1}{r^2} + O[\alpha^2 \ln^4(Mr)]. \quad (76)$$

Eq. (75) tells us that at large distances, the potential $U \propto r^{-1}$ in leading order in r , and is attracting (repelling) provided that the sign of zE is positive (negative). From Eq. (76), it follows that due to the centrifugal barrier, the potential $U \propto r^{-2}$, and is repelling at small distances. Because of a mild (logarithmic) singularity in Eq. (48), the contribution from the electric potential A_0 to the short-distance asymptotics (76) is suppressed logarithmically compared to the leading term. Furthermore, in Eq. (76), neither the leading nor sub-leading terms depend on α or z .

A characteristic feature of the potential in Eq. (74) is that it can be approximated by a relatively simple expression,

$$\bar{U} = -2E \frac{ze^2}{r} + \frac{\mu(\mu-1)}{r^2}. \quad (77)$$

For $r > M^{-1}$ ($r < M^{-1}$), the relative error of approximation (77) does not exceed 10^{-4} (10^{-2}), provided that the fine structure constant $\alpha \lesssim 1/137$. We can therefore use the approximate potential (77) to describe the bound states of the fermion-dyon system. Thus, we shall consider the approximate equation

$$\bar{u}'' + [-\varkappa^2 - \bar{U}]\bar{u} = 0, \quad (78)$$

where we use the bar to denote the approximate quantities. Based on the general considerations of [39], we can say that Eq. (73) has an infinite number of bound states for any $j \geq |q| + 1/2$, provided that $zE > 0$.

Indeed, using standard methods of the theory of differential equations, we find that for each $j \geq |q| + 1/2$, Eq. (78) possesses an infinite number of normalizable solutions

$$\bar{u}_{nj} = \mathcal{N}_{nj} (2\varkappa_{nj}r)^\mu e^{-\varkappa_{nj}r} L_n^{2\mu-1}(2\varkappa_{nj}r), \quad (79)$$

where $L_n^{2\mu-1}$ is the generalized Laguerre polynomial with the radial quantum number $n = 0, 1, 2, \dots$, \mathcal{N}_{nj} is a normalization factor, and the parameter $\varkappa_{nj} = [M^2 - \bar{E}_{nj}^2]^{1/2}$. The energies of the bound (anti)fermionic states are

$$\bar{E}_{nj} = \sigma M \left[1 + \frac{z^2\alpha^2}{(n+\mu)^2} \right]^{-1/2}, \quad (80)$$

where $\sigma = \text{sgn}(z)$ and $\mu = [(j + 1/2)^2 - q^2]^{1/2}$.

In the transition from \bar{u}_{nj} to \bar{f}_{nj} , we can neglect the term $eA_0(r)$ under the radical sign in Eq. (72a). This

is because, according to Eq. (79), noticeable changes of $\bar{u}(r)$ occur on the scale on the order of $\varkappa_{nj}^{-1} \approx (n + \mu) \times (M\alpha z)^{-1}$, whereas those of the radical $\sqrt{E + M + eA_0}$ occur on the much smaller scale on the order of M^{-1} . Due to this, the function $\bar{u}_{nj}(r)$ is still close to zero, while the radical reaches the limit of $\sqrt{E + M}$. It follows that the region $r \lesssim O[M^{-1}]$ makes no appreciable contribution to observables, and therefore the exact form there of the radical is unimportant.

Thus, we conclude that the radial wave function f_{nj} can be written approximately as

$$\bar{f}_{nj} = [\bar{E}_{nj} + M]^{1/2} \bar{u}_{nj}. \quad (81)$$

Substituting Eq. (81) into Eq. (70), we obtain an approximate expression for the radial wave function g_{nj}

$$\bar{g}_{nj} = i[\bar{E}_{nj} + M]^{-1} [\bar{f}'_{nj} - \mu \bar{f}_{nj}/r]. \quad (82)$$

Using the normalization condition $\int_0^\infty (|\bar{f}_{nj}|^2 + |\bar{g}_{nj}|^2) dr = 1$, we find that the normalization factor

$$N_{nj} = \left[1 + \frac{(n + \mu)^2}{z^2 \alpha^2} \right]^{-1/4} \left[\frac{n!}{2(n + \mu) \Gamma(n + 2\mu)} \right]^{1/2}. \quad (83)$$

In addition to the bound states of the first type, the fermion-dyon system also possesses an infinite number of bound states of the second type. The energies of these bound states are obtained from Eq. (80) by the substitution $n \rightarrow n + 1$. As a result, we have the relation $\bar{E}_{n+1j}^{(1)} = \bar{E}_{nj}^{(2)}$, from which it follows that all bound levels are doubly degenerate except for the $\bar{E}_{0j}^{(1)}$ levels. Note, however, that this twofold degeneracy takes place only within the used approximation, and is removed when corrections are taken into account.

Let us estimate the accuracy of the used approximation. To do this, we must estimate the mean value of the perturbation operator $\Delta U = U - \bar{U}$ in the state $\bar{\psi}_{nj}^{(1,2)}$. Using Eqs. (74) – (83) and approximate and analytical methods, we can show that $\langle \Delta U \rangle_{nj} \propto Mz^4 \alpha^4$. Using the results obtained for the hydrogen atom, we can assume that the radiative corrections ΔE_{rad} to the bound (anti)fermionic levels are $\propto Mz^4 \alpha^5 \ln(1/\alpha)$. In view of the above, we conclude that Eq. (80) is only valid up to terms of order $z^2 \alpha^2$, and hence can be rewritten as

$$\bar{E}_{nj} = \sigma M \left[1 - \frac{z^2 \alpha^2}{2(n + \mu)^2} \right]. \quad (84)$$

The relative error of Eq. (84) is on the order of $z^2 \alpha^2$. We see that in the most interesting case of $|q| = 1/2$ and $\alpha \approx 1/137$, this error is on the order of $0.005 \div 0.01\%$.

The difference between E_{nj} obtained by numerical methods and \bar{E}_{nj} of Eq. (84) is in agreement with this estimate.

Eqs. (81) and (82) were obtained under the assumptions $E > 0$ and $\sigma = \text{sgn}(z) = 1$. The approximate antifermionic wave functions are obtained from Eqs. (81) and (82) via the substitution (CP inversion)

$$\bar{f}_{nj} \rightarrow -i\bar{g}_{nj}, \bar{g}_{nj} \rightarrow i\bar{f}_{nj}, \bar{E}_{nj} \rightarrow -\bar{E}_{nj}. \quad (85)$$

Note that substitution (85) converts fermionic states of the first (second) type into antifermionic states of the second (first) type.

The approximated energy spectrum (80) is hydrogen-like. Formally, the spectrum of the hydrogen atom is obtained from Eq. (80) by the substitution $z \rightarrow 1$, $q \rightarrow \alpha$. However, the angular momentum j is half-integral for the hydrogen atom, whereas, it is an integer (half-integer) for the fermion-dyon system, provided that q is a half-integer (integer). The approximated spectrum (80) is similar to the exact spectrum of a fermion-dyon system obtained in [25–28] for the case of the Coulomb electric potential and nonminimal angular momenta $j \geq |q| + 1/2$. This spectrum can be obtained from Eq. (80) by the substitution $z \rightarrow Z_D$, $q^2 \rightarrow q^2 + (Z_D \alpha)^2$, where Z_D is an integer, and $Z_D e$ is the dyon's charge.

The energy levels of the Coulomb fermion-dyon system are doubly degenerate, satisfying the relation $E_{nj}^{(1)} = E_{nj}^{(2)}$. Unlike the twofold degeneracy of the fermion-dyon system considered here, the twofold degeneracy of the Coulomb fermion-dyon system is exact at the quantum mechanical level, but it is probably removed by radiative corrections. This exact quantum mechanical twofold degeneracy is a consequence of the Coulomb electric potential used in [25–28]. In our case, the electric potential is essentially non-Coulomb for $r \lesssim M^{-1}$, and due to this, the twofold degeneracy of the energy levels is removed already at the quantum mechanical level.

The rich structure of the energy levels of the fermion-dyon system considered here implies the possibility of numerous radiative transitions between them. It is similar with the hydrogen atom, but there is an important difference: because of the violation of parity, the electric dipole transitions with $\Delta j = 0$ are allowed for a fermion-dyon system [28, 31], as well as $\Delta j = \pm 1$ transitions, unlike for the hydrogen atom, where parity conservation strictly forbids $\Delta j = 0$ transitions and allows only $\Delta j = \pm 1$ transitions.

Another difference from the hydrogen atom is the tightly bound state of the fermion-dyon system. In the general case, the binding energy of this state exceeds those of the loosely bound states by orders of magnitude. As a result, the energy of a photon emitted by

a transition from a loosely bound state to the tightly bound state exceeds by orders of magnitude the energies of photons emitted by transitions between loosely bound states. In contrast, there is no analog of the tightly bound state of the fermion-dyon system in the hydrogen atom, and therefore the maximum possible energy of an emitted photon is of the same order of magnitude as the energies of some other emitted photons.

5 Electric dipole moments of the bound fermionic states

It was shown in Section 2 that P transformation changes sign of the magnetic charge of the monopole, and therefore cannot be a symmetry of the fermion-monopole system. In particular, the bound fermionic states are not eigenstates of P transformation. This makes it possible for the bound states of the fermion-dyon system to have a nonzero electric dipole moment. On the contrary, if a bound fermionic state is an eigenstate of P , as is the case for the hydrogen atom, then it cannot possess a nonzero electric dipole moment. This is because the electric dipole moment operator $\mathbf{d} = e\mathbf{r}$ changes sign under P transformation, whereas the bound fermionic state remains unchanged modulo a phase factor.

It follows from the conservation of angular momentum that the only nonvanishing component of the operator \mathbf{d} in a state ψ_{jm} is the z component

$$\langle d_z \rangle_{jm} = e \int \psi_{jm}^\dagger z \psi_{jm} d^3x. \quad (86)$$

It was shown in Section 4 that the induced electric charge of the dyon results in the existence of an infinite number of bound fermionic states for each admissible value j of the angular momentum. Each bound state of the fermion-dyon system possesses a nonzero electric dipole moment, provided that $|q| > 1/2$. We shall consider the cases of bound fermionic states with the minimal ($j = |q| - 1/2$) and nonminimal ($j \geq |q| + 1/2$) angular momentum separately.

5.1 Electric dipole moments of the bound fermionic states with the angular momentum $j = |q| - 1/2$

In this case, the bound fermionic states are of the third type, and the expression of the electric dipole moment takes the form

$$\langle d_z \rangle_{jm} = e \int \eta_{jm}^\dagger \eta_{jm} \cos(\vartheta) d\Omega \int_0^\infty r(|f|^2 + |g|^2) dr. \quad (87)$$

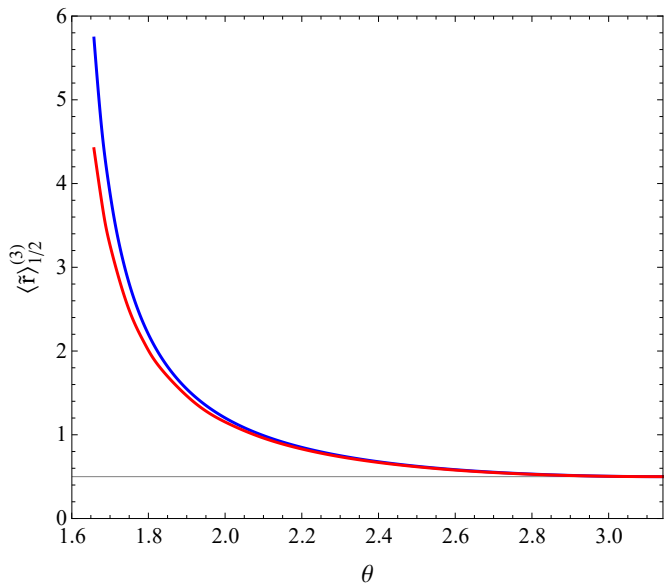


Fig. 4 Dependence of the dimensionless mean radius of the fermion spatial distribution $\langle \tilde{r} \rangle_{1/2}^{(3)} = M \langle r \rangle_{1/2}^{(3)}$ on the parameter θ . The red (blue) curve is obtained with (without) taking into account the electric charge of the dyon. The curves correspond to the parameters $\alpha = 1/137$ and $q = 1$

It was shown in [14] that the kinematic factor

$$\int \eta_{jm}^\dagger \eta_{jm} \cos \vartheta d\Omega = -\text{sgn}(q) \frac{m}{j+1}, \quad (88)$$

where the angular momentum $j = |q| - 1/2$ and the z projection $m \in [-|q| + 1/2, |q| - 1/2]$. Note that the kinematic factor vanishes in the important case of $q = \pm 1/2$, which corresponds to the elementary (the winding number $n = \pm 1$) magnetic (anti)monopole.

Substituting the radial wave functions from Eq. (38) into the second integral in Eq. (87), and using Eq. (88), we obtain an analytical expression for the electric dipole moment of the unperturbed bound state (38)

$$\langle d_z \rangle_{jm} = -\text{sgn}(q) \frac{m}{j+1} \frac{e}{2M |\cos \theta|}. \quad (89)$$

Eq. (89) tells us that the electric dipole moment of the unperturbed state (38) increases indefinitely $\propto (\pi/2 - |\theta|)^{-1}$ as $|\theta| \rightarrow \pi/2$. The reason is that in this limit, the state (38) becomes loosely bound, and therefore the fermion is weakly localized. In contrast, the state (38) is tightly bound when $|\theta|$ is in the neighbourhood of π . In this case, the radial integral in Eq. (87) is on the order of the Compton wavelength of the fermion, and the dipole moment reaches its minimum values.

Eq. (89) is obtained without accounting for the electric charge of the dyon. To account for it, we must solve the Dirac equation with the perturbed Hamiltonian (56) and substitute the obtained radial wave functions into Eq. (87). To solve the Dirac equation, we

use numerical methods of the MATHEMATICA software package [40].

It follows from Eq. (87) that the electric dipole moment is proportional to the mean radius of the fermion spatial distribution $\langle r \rangle_j^{(3)} = \int_0^\infty r(|f_j|^2 + |g_j|^2) dr$, where the type and angular momentum of the fermionic state are indicated. Figure 4 shows the dependence of the dimensionless mean radius $\langle \tilde{r} \rangle_j^{(3)} = M \langle r \rangle_j^{(3)}$ on the parameter θ for two cases. In the first case, the contribution of the dyon's electric charge was taken into account, whereas in the second case it was not. It follows from Eq. (89) that in the second case, the mean radius $\langle \tilde{r} \rangle_j^{(3)} = 2^{-1} |\cos(\theta)|^{-1}$, and it does not depend on j . In contrast, $\langle r \rangle_j^{(3)}$ depends on j when the contribution of the dyon electric charge is taken into account. The reason is that the dyon's electric charge (42) is proportional to q , and the angular momentum $j = |q| - 1/2$ for the fermionic states of the third type. In Fig. 4, the parameter $q = 1$, which corresponds to the angular momentum $j = 1/2$. In this case, the z projection $m = -1/2, 1/2$ and the electric dipole moment is different from zero.

From Fig. 4 it follows that taking into account the dyon's electric charge leads to a decrease in the mean radius of the fermion distribution, which results in a decrease in the magnitude of the electric dipole moment. The reason is that the electric potential (46) is attractive for all values of θ in Fig. 4. Further, it follows from Fig. 4 that the correction to the dipole moment (89) caused by the electric charge of the dyon is insignificant when the state (38) is tightly bound. In contrast, these corrections become substantial for loosely bound states, i.e. for $|\theta| = \pi/2 + \epsilon$, where $\epsilon \ll 1$. This is because in this region of θ , the contribution of the electric potential A_0 to the forming of the fermionic bound state becomes comparable to the contribution of the boundary condition (34).

It was shown in subsection 4.1 that in addition to the state (38), which is tightly bound in general, there is also an infinite sequence of loosely bound states. Being fermionic states of the third type, they possess the minimum possible angular momentum $j = |q| - 1/2$. To find the mean radii $\langle r \rangle_{nj}^{(3)}$ of these states, we use the numerical methods of subsection 4.1. First, we find the combination $F_{nj}(r) = f_{nj}(r) - i \tan[\theta/2 + \pi/4] g_{nj}(r)$ that satisfies the homogeneous Dirichlet boundary conditions. Knowing F_{nj} and using the system (23), we can express the radial wave functions f_{nj} and g_{nj} as linear combinations of F_{nj} and its derivative F'_{nj} , and then calculate the corresponding mean radius $\langle r \rangle_{nj}^{(3)}$.

Figure 5 presents the dependence of the dimensionless mean radius $\langle \tilde{r} \rangle_{n1/2}^{(3)} = M \langle r \rangle_{n1/2}^{(3)}$ on the parameter

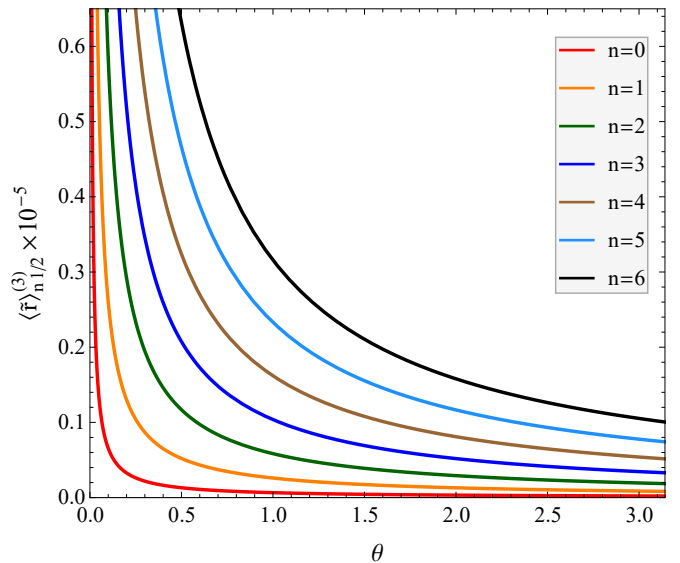


Fig. 5 Dependence of the dimensionless mean radius $\langle \tilde{r} \rangle_{n1/2}^{(3)} = M \langle r \rangle_{n1/2}^{(3)}$ on θ for the first few values of the radial quantum number n . The curves correspond to the parameters $\alpha = 1/137$ and $q = 1$

θ for the first few values of the radial quantum number n . It was found that in Fig. 5, the curves $\langle \tilde{r} \rangle_{n1/2}^{(3)}$ can be approximated by the hyperbolas

$$\langle \tilde{r} \rangle_{n1/2}^{(3)} \approx a_{n1/2}^{(3)} \theta^{-1} \quad (90)$$

with an accuracy of $\sim 0.1\%$. The coefficient $a_{n1/2}^{(3)}$ increases monotonically (approximately $\propto n(n+b)$, where b is a constant) with an increase in the radial quantum number n . Note that the radial quantum number n is equal to the number of zeros of the function $F_{nj} = f_{nj} - i \tan[\theta/2 + \pi/4] g_{nj}$ except for the zero at $r = 0$. At the same time, all zeros of the radial wave functions f_{nj} and g_{nj} are at nonzero r , and there are $n+1$ of them. The behaviour and the scale of the curves in Fig. 5 are similar to those for the curves shown in Fig. 6, and will be explained in the next subsection.

5.2 Electric dipole moments of the bound fermionic states with the angular momentum $j \geq |q| + 1/2$

It was shown in [14] that in this case, the electric dipole moment is

$$\langle d_z \rangle_{njm} = -\frac{mq}{j(j+1)} e \langle r \rangle_{nj}, \quad (91)$$

where the mean radius of the fermion distribution

$$\langle r \rangle_{nj} = \int_0^\infty r(|f_{nj}|^2 + |g_{nj}|^2) dr \quad (92)$$

and the z projection $m \in [-j, j]$. In contrast to the previous case $j = |q| - 1/2$, the dipole moment (91)

differs from zero even if $q = \pm 1/2$, since the angular momentum j is now greater than zero. Eq. (91) tells us that all dependence of $\langle d_z \rangle_{njm}$ on θ is contained in the mean radius $\langle r \rangle_{nj}$.

Figure 6 presents the dependence of the dimensionless mean radius $\langle \tilde{r} \rangle_{n1}^{(1)} = M \langle r \rangle_{n1}^{(1)}$ on θ for the radial quantum numbers $n = 0, \dots, 6$. The results correspond to the bound fermionic states of the first type $\psi_{n1m}^{(1)}$. All the curves in Fig. 6 are approximated with high accuracy by the hyperbolas $a_{n1}^{(1)}/\theta$, where the coefficients $a_{n1}^{(1)}$ increase monotonically with an increase in n . The same pattern also holds for fixed n and increasing j . In this case, the curves are approximated by the hyperbolas $a_{nj}^{(1)}/\theta$ with the coefficients $a_{nj}^{(1)}$ monotonically increasing with an increase in j . Similar results hold for the bound fermionic states of the second type $\psi_{njm}^{(2)}$. In particular, in this case, the mean radius $\langle r \rangle_{nj}^{(2)}$ is also inversely proportional to the parameter θ and increases monotonically with an increase in n or j .

The hyperbolic θ -dependence of the curves in Fig. 6 can be obtained from the approximate solution (79) – (83). Indeed, by substituting $r = \varkappa_{nj}^{-1} \rho$ in integral (92) and using Eqs. (79) – (83), we can show that $\langle r \rangle_{nj}^{(1)} \propto \varkappa_{nj}^{-1}$ up to corrections of order α^2 . We see that in the leading order in α , the dependence of $\langle r \rangle_{nj}^{(1)}$ on the parameter θ is isolated in \varkappa_{nj} . Using Eq. (80) and the definition $\varkappa_{nj} = (M^2 - E_{nj}^2)^{1/2}$, we find that $\varkappa_{nj}^{-1} = \pi(n + \mu) / (M\alpha q\theta) + O[\alpha]$. Hence, in the leading order in α , $\varkappa_{nj}^{-1} \propto \theta^{-1}$, which explains the hyperbolic θ -dependence of the curves in Fig. 6.

Using the approximate solution (79) – (83), one can obtain the asymptotics of $\langle r \rangle_{nj}$ for large n or j . In particular, for large n and fixed j , we find that

$$\langle r \rangle_{nj}^{(a)} \sim (bn + c^{(a)}(\mu))(n + \mu) / (Mz\alpha), \quad (93)$$

where b is a positive constant of the order of unity, $c^{(a)}(\mu)$ is an increasing quasilinear function of the parameter $\mu = [(j + 1/2)^2 - q^2]^{1/2}$, $z = q\theta/\pi$, and the index $a = 1(2)$ for the fermionic states of the first (second) type. Similarly, for large j and fixed n , we find that

$$\langle r \rangle_{nj}^{(a)} \sim j(j + 3n + a + 1/2) / (Mz\alpha). \quad (94)$$

A comparison of Figs. 4 and 6 shows that the mean radius $\langle r \rangle_{nj}^{(1)}$ significantly (approximately by four orders of magnitude) exceed the mean radius $\langle r \rangle^{(3)}$ of the bound state (38). The reason is that the existence of the bound state (38) is caused by the boundary condition (34), whereas the existence of the bound states $\psi_{njm}^{(1)}$ is entirely due to the electric charge of the dyon. As a result, the mean radius $\langle r \rangle_{nj}^{(1)} \approx F^{(1)}(n, j) \varkappa_{nj}^{-1} \approx$

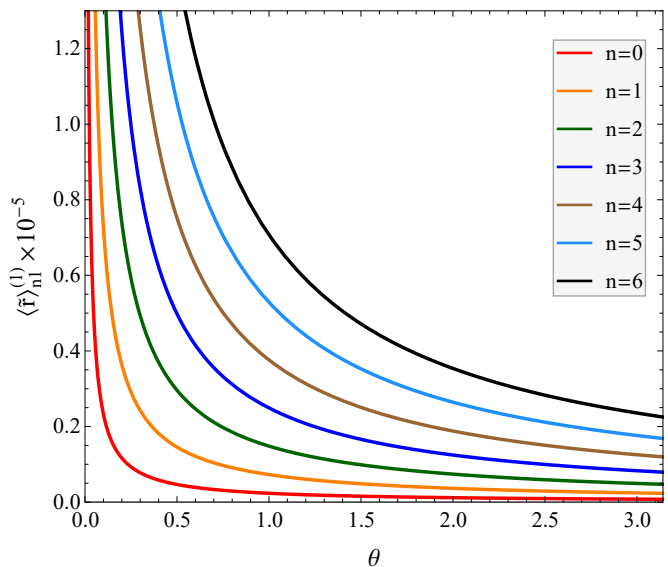


Fig. 6 Dependence of the dimensionless mean radius $\langle \tilde{r} \rangle_{nj}^{(1)} = M \langle r \rangle_{nj}^{(1)}$ on θ for the angular momentum $j = 1$ and the radial quantum numbers $n = 0, \dots, 6$. The curves correspond to the parameters $\alpha = 1/137$ and $q = 1/2$

$F^{(1)}(n, j) \times (n + \mu) \pi / (M\alpha q\theta)$, where $F^{(1)}(n, j)$ is a function of n and j . We see that $\langle r \rangle_{nj}^{(1)}$ is proportional to the large factor $\pi/(\alpha q) \approx 860$, whose large magnitude is due to the smallness of the fine structure constant $\alpha = 1/137$. The remaining factor $F^{(1)}(n, j)(n + \mu)$ is on the order of $10 \div 20$. In contrast, for the unperturbed bound state (38), the mean radius $\langle r \rangle^{(3)} = (2M |\cos(\theta)|)^{-1}$, and accounting for the Coulomb correction does not lead to a qualitative change in the situation. We see that in contrast to $\langle r \rangle_{nj}^{(1)}$, the mean radius $\langle r \rangle^{(3)}$ does not contain a large multiplier $\propto \alpha^{-1}$. This explains the difference in the magnitudes of $\langle r \rangle_{nj}^{(1)}$ and $\langle r \rangle^{(3)}$. The difference in the magnitudes of $\langle r \rangle_{nj}^{(2)}$ and $\langle r \rangle^{(3)}$ is explained similarly.

Due to the nonzero electric dipole moments, the energy levels of the fermion-dyon system are split in an external homogeneous electric field (Stark effect). This splitting removes the degeneracy with respect to the z -projection m of the angular momentum. Because of the difference in the mean radii $\langle r \rangle_{nj}^{(1,2)}$ and $\langle r \rangle^{(3)}$, the splitting of the tightly bound levels, which is possible only if $|q| > 1/2$, will be much smaller than that of the loosely bound levels.

6 Magnetic dipole moments of the bound fermionic states

The operator of magnetic moment is

$$\boldsymbol{\mu} = \frac{e}{2} \mathbf{r} \times \boldsymbol{\alpha}. \quad (95)$$

It follows from Eq. (95) that $\boldsymbol{\mu}$ is an axial-vector operator. Using Eqs. (20) and (95), it is easy to show that the magnetic dipole moment of the fermionic states of the third type vanishes [14]. Indeed, there exists only one two-component angular eigensection η_{qm} when $j = |q| - 1/2$. As a result, the two cross terms produced by the matrix $\boldsymbol{\alpha}$ in $\boldsymbol{\mu}$, have the same angular structure $\eta_{qm}^\dagger (\mathbf{r} \times \boldsymbol{\sigma}) \eta_{qm}$. It is known [11] that η_{qm} is an eigensection of the operator $\mathbf{r} \cdot \boldsymbol{\sigma}$ with the eigenvalue $q/|q|$. At the same time, the operator $\mathbf{r} \cdot \boldsymbol{\sigma}$ anticommutes with the operator $\mathbf{r} \times \boldsymbol{\sigma}$. It follows that the dipole magnetic moment $\boldsymbol{\mu}$ vanishes for the bound fermionic states of the third type.

In contrast, the magnetic dipole moment is different from zero for the bound states of the first and second types. It was shown in [14] that in this case, the magnetic dipole moment is

$$\langle \mu_z \rangle_{njm}^{(a)} = (-1)^{a+1} \frac{e}{2} \frac{m\mu}{j(j+1)} \int_0^\infty r (i f_{nj}^* g_{nj}) dr, \quad (96)$$

where $\mu = [(j+1/2)^2 - q^2]^{1/2}$, and the index $a = 1$ (2) for a state of the first (second) type. Numerical calculations reveal that the dipole moment $\langle \mu_z \rangle_{njm}^{(a)}$ is practically independent of the parameter θ . Analytical calculations performed with the use of approximate solutions of Section 4 show that in the leading order in $z\alpha$, the dipole moment

$$\langle \mu_z \rangle_{njm}^{(a)} \approx \frac{e}{8M} \frac{m\mu}{j(j+1)} (1 + (-1)^{a+1} 2\mu). \quad (97)$$

Eq. (97) is independent of θ , and describes the numerical results with high accuracy.

The absence of the θ -dependence of the dipole magnetic moment $\langle \mu_z \rangle_{njm}^{(a)}$ is explained by the presence of the cross term f^*g in Eq. (96). Indeed, the system of equations (70) and (71) tells us that in leading order in α , the radial function $g_{nj} \approx i (f'_{nj} \mp \mu f_{nj}/r) / (2M)$, where the upper (lower) sign corresponds to a state of the first (second) type. Further, Eqs. (79) and (80) tell us that the approximate solution f_{nj} depends on r only through the dimensionless combination $\rho = \varkappa_{nj} r$. Expressing the radial function g_{nj} in terms of f_{nj} and making the substitution $r = \varkappa_{nj}^{-1} \rho$, we conclude that in Eq. (96), the dependence of the integral $\int_0^\infty r (i f^* g) dr$ on θ is isolated in the factor $\mathcal{N}_{nj}^2 \varkappa_{nj}^{-1}$. Using the formulae of Section 4, it is easy to show that this factor does not depend on either θ or α . This explains the independence of the dipole moment $\langle \mu_z \rangle_{njm}^{(a)}$ of θ in the leading (zero) order in α .

It follows from the above that the θ -dependences of the dipole moments $\langle d_z \rangle_{njm}^{(a)} \propto \theta^{-1}$ and $\langle \mu_z \rangle_{njm}^{(a)} \propto \theta^0$ are completely different. Furthermore, numerical calculations and Eq. (97) tell us that $\langle \mu_z \rangle_{njm}^{(a)}$ is independent of the radial quantum number n . In contrast, it

follows from Fig. 6 and Eqs. (93) and (94) that $\langle d_z \rangle_{njm}^{(a)}$ increases monotonically with an increase in n . At the same time, Eqs. (91), (94), and (97) tell us that for large values of j , both $\langle \mu_z \rangle_{njm}^{(a)}$ and $\langle d_z \rangle_{njm}^{(a)}$ cease to depend on j while remaining proportional to the z projection m . Finally, in the leading order in α , the electric dipole moment $\langle d_z \rangle_{njm}^{(a)} \propto \alpha^{-1}$, whereas the magnetic dipole moment $\langle \mu_z \rangle_{njm}^{(a)} \propto \alpha^0$. As a result, for a given state, the magnitude of the electric dipole moment significantly exceeds the magnitude of the magnetic dipole moment. These significant differences between $\langle d_z \rangle_{njm}^{(a)}$ and $\langle \mu_z \rangle_{njm}^{(a)}$ are due to the different structures of the radial integrals in Eqs. (91) and (96).

Like a homogeneous electric field, a homogeneous magnetic field removes the degeneracy of the energy levels of the fermion-dyon system with respect to the quantum number m (Zeeman effect). The splitting is only possible for the states with the angular momenta $j \geq |q| + 1/2$, since the magnetic dipole moment of a bound fermionic state vanishes otherwise.

7 Conclusion

In this paper, we have studied the bound fermionic states in the external field of an Abelian dyon, which is the Dirac monopole surrounded by the cloud of an induced electric charge. The fermion-monopole system has several characteristic properties. In particular, the magnetic field of the monopole changes sign under P transformation, which is equivalent to the change of sign of the monopole's magnetic charge. Since C conjugation also changes the sign of the monopole's magnetic charge, combined CP transformation leaves the monopole's magnetic field unchanged. From this, one could naively conclude that CP is a symmetry of the fermion-monopole system. However, there is one obstacle that makes this impossible. The absence of the centrifugal barrier in the states with the minimal angular momentum $j = |q| - 1/2$ leads to the fact that the Dirac Hamiltonian is not self-adjoint on these states.

To solve this problem, a boundary condition must be imposed so that the Dirac Hamiltonian possesses a complete set of eigenfunctions. The appropriate boundary condition at $r = 0$ forms a one-parameter family of self-adjoint extensions of the Dirac Hamiltonian [13, 15]. Thus, in addition to the Hamiltonian, the fermion-soliton system is characterized by an angular parameter θ entering into the boundary condition. The parameter θ defined modulo 2π results in the existence of the θ vacua.

Although CP leaves the magnetic field of the monopole unchanged, it changes sign of the parameter θ . In the

case of massive fermions, this results in a breaking of CP invariance of the fermion-monopole system. This makes possible the appearance of the electric charge of the monopole via quantum effects (polarization of the fermionic vacuum), since the spherically symmetric electric field is also not invariant (it changes sign) under CP .

Indeed, it has been shown in [16] that the polarization of the fermionic vacuum in the vicinity of the Dirac monopole leads to the appearance of a spherically symmetric electric charge density. Because of the mild integrable singularity $\propto r^{-2} \ln(Mr)$ of the electric charge density at the origin, the electrostatic energy of the electric charge distribution is finite. The electric charge for a unit monopole obeys the Witten formula $Q = -e\theta/2\pi$ so that the monopole becomes a dyon. At spatial infinity, the dyon's electric potential is asymptotically Coulombic ($\sim Q/r$), but it differs significantly from the Coulomb potential when $r \lesssim M^{-1}$.

The nontrivial boundary condition at $r = 0$ results in a bound fermionic state [13, 15] possessing the minimal angular momentum $j = |q| - 1/2$. In the general case, this state is tightly bound. The consideration of the dyon's electric field leads to a shift in the energy of this bound state resulting in an increase in the magnitude of the binding energy.

In addition to perturbing the already existing tightly bound state, the dyon's electric field leads to the appearance of new bound states. These states are loosely bound, and there are an infinite number of them for each value of the angular momentum, including the minimum possible value $j = |q| - 1/2$. In the latter case, to ensure the Hermiticity of the Dirac Hamiltonian, the fermionic wave functions must satisfy the boundary condition (34), which remains unchanged due to the weak logarithmic singularity of the electric potential. At the same time, the point distribution of the electric charge density $\rho(\mathbf{r}) = Q\delta(\mathbf{r})$ leads to a falling of the fermion on the centre, which is unacceptable from a physical viewpoint. Furthermore, the boundary condition (34) is incompatible with such a behaviour of the fermion.

Because of the centrifugal barrier, there is no need for a boundary condition at $r = 0$ for the states with the nonminimal angular momenta $j \geq |q| + 1/2$. In this case, an analytical approximation of the potential is possible, which allows us to find the solution to the Dirac equation in an analytical form. The approximated analytical spectrum is hydrogen-like and resembles the exact analytical spectrum for a purely Coulomb fermion-dyon system [25–28].

Since the fermion-dyon system is not invariant under P transformation, all its bound states have nonzero

electric dipole moments, which distinguishes it from the hydrogen atom. These electric dipole moments depend nontrivially on the parameter θ . The analytical approximate solution for the bound states with the angular momenta $j \geq |q| + 1/2$ makes it possible to find the asymptotics of the electric dipole moments for large values of j . In the most interesting case of $|q| = 1/2$, the minimum angular momentum $j = |q| - 1/2$ vanishes, which results in the vanishing of the dipole moment of the corresponding bound state.

The bound states with nonminimal angular momenta possess nonzero magnetic dipole moments. In contrast, the magnetic dipole moments vanish for the bound states with the minimal angular momentum $j = |q| - 1/2$, which may ($|q| = 1/2$) or may not ($|q| > 1/2$) be zero. Unlike the electric dipole moments, the magnetic dipole moments are practically independent of the parameter θ . Also, for a given state, the magnitude of the electric dipole moment is much larger than that of the magnetic dipole moment. These differences are caused by the different structures of the radial integrals determining the values of these two moments.

Acknowledgements This work was supported by the Russian Science Foundation, grant No 23-11-00002.

References

1. P. A. M. Dirac, Proc. R. Soc. London A **133**, 60 (1931) <https://doi.org/10.1098/rspa.1931.0130>
2. P. A. M. Dirac, Phys. Rev. **74**, 817 (1948) <https://doi.org/10.1103/PhysRev.74.817>
3. I. Tamm, Z. Phys. **71**, 141 (1931) <https://doi.org/10.1007/BF01341701>
4. M. Fierz, Helv. Phys. Acta **17**, 27 (1944)
5. P. P. Banderet, Helv. Phys. Acta **19**, 503 (1946)
6. Harish-Chandra, Phys. Rev. **74**, 883 (1948) <https://doi.org/10.1103/PhysRev.74.883>
7. C. A. Hurst, Ann. Phys. (N.Y.) **50**, 51 (1968) [https://doi.org/10.1016/0003-4916\(68\)90316-3](https://doi.org/10.1016/0003-4916(68)90316-3)
8. M. Berrondo, H. V. McIntosh, J. Math. Phys. **11**, 125 (1970) <https://doi.org/10.1063/1.1665037>
9. T. T. Wu, C. N. Yang, Nucl. Phys. B **107**, 365 (1976) [https://doi.org/10.1016/0550-3213\(76\)90143-7](https://doi.org/10.1016/0550-3213(76)90143-7)
10. T. T. Wu, C. N. Yang, Phys. Rev. D **16**, 1018 (1977) <https://doi.org/10.1103/PhysRevD.16.1018>
11. Y. Kazama, C. N. Yang, A. S. Goldhaber, Phys. Rev. D **15**, 2287 (1977) <https://doi.org/10.1103/PhysRevD.15.2287>
12. Y. Kazama, C. N. Yang, Phys. Rev. D **15**, 2300 (1977) <https://doi.org/10.1103/PhysRevD.15.2300>
13. A. S. Goldhaber, Phys. Rev. D **16**, 1815 (1977) <https://doi.org/10.1103/PhysRevD.16.1815>
14. Y. Kazama, Phys. Rev. D **16**, 3078 (1977) <https://doi.org/10.1103/PhysRevD.16.3078>
15. C. J. Callias, Phys. Rev. D **16**, 3068 (1977) <https://doi.org/10.1103/PhysRevD.16.3068>
16. H. Yamagishi, Phys. Rev. D **27**, 2383 (1983) <https://doi.org/10.1103/PhysRevD.27.2383>

17. P. Osland, T. T. Wu, Nucl. Phys. B **247**, 421 (1984) [https://doi.org/10.1016/0550-3213\(84\)90557-1](https://doi.org/10.1016/0550-3213(84)90557-1)
18. P. Osland, T. T. Wu, Nucl. Phys. B **247**, 450 (1984) [https://doi.org/10.1016/0550-3213\(84\)90558-3](https://doi.org/10.1016/0550-3213(84)90558-3)
19. P. Osland, T. T. Wu, Nucl. Phys. B **256**, 13 (1985) [https://doi.org/10.1016/0550-3213\(85\)90383-9](https://doi.org/10.1016/0550-3213(85)90383-9)
20. P. Osland, T. T. Wu, Nucl. Phys. B **256**, 32 (1985) [https://doi.org/10.1016/0550-3213\(85\)90384-0](https://doi.org/10.1016/0550-3213(85)90384-0)
21. P. Osland, C. L. Schultz, T. T. Wu, Nucl. Phys. B **256**, 449 (1985) [https://doi.org/10.1016/0550-3213\(85\)90404-3](https://doi.org/10.1016/0550-3213(85)90404-3)
22. P. Osland, T. T. Wu, Nucl. Phys. B **261**, 687 (1985) [https://doi.org/10.1016/0550-3213\(85\)90594-2](https://doi.org/10.1016/0550-3213(85)90594-2)
23. S. K. Bose, J. Phys. G **12**, 1135 (1986) <https://doi.org/10.1088/0305-4616/12/11/005>
24. X.-Z. Li, K.-L. Wang, J.-Z. Zhang, Phys. Lett. B **148**, 89 (1984) [https://doi.org/10.1016/0370-2693\(84\)91616-2](https://doi.org/10.1016/0370-2693(84)91616-2)
25. X.-Z. Li, J.-Z. Zhang, Phys. Rev. D **33**, 562 (1986) <https://doi.org/10.1103/PhysRevD.33.562>
26. P. H. Frampton, J.-Z. Zhang, Y.-C. Qi, Phys. Rev. D **40**, 3533 (1989) <https://doi.org/10.1103/PhysRevD.40.3533>
27. J.-Z. Zhang, Y.-C. Qi, J. Math. Phys. **33**, 1796 (1990) <http://dx.doi.org/10.1063/1.528677>
28. J.-Z. Zhang, Phys. Rev. D **41**, 1280 (1990) <https://doi.org/10.1103/PhysRevD.41.1280>
29. X.-Z. Li, J.-Z. Zhang, J. Phys. A **26**, 4451 (1993) <https://doi.org/10.1088/0305-4470/26/17/049>
30. J.-Z. Zhang, Phys. Lett. B **532**, 215 (2002) [https://doi.org/10.1016/S0370-2693\(02\)01535-6](https://doi.org/10.1016/S0370-2693(02)01535-6)
31. E. A. Tolkachev, L. M. Tomil'chik, Ya. M. Shnir, J. Phys. G **14**, 1 (1988) <https://doi.org/10.1088/0305-4616/14/1/004>
32. Ya. M. Shnir, E. A. Tolkachev, L. M. Tomil'chik, Int. J. Mod. Phys. A **7**, 3747 (1992) <https://doi.org/10.1142/S0217751X92001666>
33. S. G. Kovalevich, Ya. M. Shnir, E. A. Tolkachev, Physica Scripta **53**, 51 (1996) <https://doi.org/10.1088/0031-8949/53/1/009>
34. T. T. Wu, C. N. Yang, Phys. Rev. D **12**, 3845 (1975) <https://doi.org/10.1103/PhysRevD.12.3845>
35. E. Witten, Phys. Lett. **86B**, 283 (1979) [https://doi.org/10.1016/0370-2693\(79\)90838-4](https://doi.org/10.1016/0370-2693(79)90838-4)
36. F. Wilczek, Phys. Rev. Lett. **48**, 1146 (1982) <https://doi.org/10.1103/PhysRevLett.48.1146>
37. R. Jackiw, C. Rebbi, Phys. Rev. D **13**, 3398 (1976) <https://doi.org/10.1103/PhysRevD.13.3398>
38. F. W. J. Olver, D. W. Lozier, R. F. Boisvert, C. W. Clark, eds., *NIST Handbook of Mathematical Functions*, (Cambridge University Press, Cambridge, 2010)
39. L. D. Landau, E. M. Lifshitz, *Quantum Mechanics: Non-Relativistic Theory. Vol. 3*, (3rd ed.) (Pergamon Press, Oxford, 1977)
40. Wolfram Research, Inc., Mathematica, Version 12.2. Champaign, IL (2020) <https://www.wolfram.com>